

## **COST-EFFECTIVE GEOMETRICALLY NONLINEAR FE-FORMULATION FOR SOFT TISSUES' DEFORMATION**

*UDC 515.3 : 519.853*

**Dragan Marinković<sup>1,2</sup>, Katja Joechen<sup>3</sup>**

<sup>1</sup>Institut für Mechanik, TU Berlin, Straße des 17. Juni, 10623 Berlin, Deutschland

<sup>2</sup>Mechanical Engineering Faculty, University of Niš, A. Medvedeva 14, 18000 Niš, Serbia

<sup>3</sup>Institut für Technische Mechanik, Universität Karlsruhe (TH), Kaiserstr. 10, 76131 Karlsruhe, Deutschland

E-mail: Dragan.Marinkovic@TU-Berlin.de

**Abstract.** *Accurate prediction of the behavior of soft bodies' deformation is a demanding task, since it involves geometrical and material nonlinearities as well as variable boundary conditions, i.e. contact problems. This paper represents the first step in handling the issue by proposing development of cost-effective 3D finite element for analyzing geometrical-only nonlinear deformations. The proposed geometrically nonlinear formulation is of the updated Lagrange type and can relatively easily be extended so as to account for other nonlinear aspects (material nonlinearities, contact). It also represents a good compromise between the numerical effort and achieved accuracy. A set of examples, starting from very simple ones and going toward more complex ones, is given to demonstrate the application of developed element and formulation.*

**Key Words:** *Finite Element Method, Geometrically Nonlinear Analysis, Tetrahedron Element*

### 1. INTRODUCTION

Modeling of deformable structures is one of the primary tasks in mechanical engineering, with the main objective to predict the response of structures under the influence of predefined static and/or transient loads with high accuracy. Typical engineering materials (such as steel, metal alloys, composites, etc) are characterized by very high stiffness and structures made of those materials exhibit in praxis relatively small deformations. In majority of cases deformations are small enough to allow engineers to make significant simplifications and perform their calculations in the field of linear analysis, still achieving the required level of accuracy.

Nevertheless, modeling the behavior of soft materials, such as tissues, foam materials, etc. has gained in importance over the last decade. On the one hand, a number of research

groups dedicate their work to development of various surgical simulators (e.g. [4, 5]). Development of such a device is a multidisciplinary task with one of the most important demands to develop models that can give satisfactorily accurate representation of the internal organ mechanics, while still allowing real-time computation – two requirements which are not easy to conciliate. On the other hand, there are research groups that concentrate their efforts on evaluation of accurate mechanical characteristics of soft tissues (e.g. [7, 8]). Various approaches have been used in both research fields, but the finite element method (FEM), as a most powerful tool in structural analysis, appears to be predominant one. However, significant differences with respect to typical mechanical structures arise from the fact that the considered soft materials exhibit highly and therefore non-negligible nonlinear behavior, which has its origins in both material and geometrical nonlinearities, as well as contact.

The authors of the paper propose a linear tetrahedral 3D finite element, which has good adaptability to various geometries. In the first step, it is aimed at geometrically nonlinear formulation, whereby it is kept in mind that the final aim is a fully nonlinear formulation. Furthermore, it is also aimed at a flexible formulation, in which balancing between the computational effort and achieved accuracy can be performed. The nature of this trade-off is not trivial and the proposed formulation may provide some insight into the matter.

## 2. GEOMETRICALLY NONLINEAR FORMULATION

The prediction of the linearity of the system response rests on assumptions of rather small displacements compared to dimensions of the modeled object, linear elastic material behavior and invariability of boundary conditions. Those are only approximations of the real behavior, but generally speaking, none of them is applicable to the deformational behavior of soft tissues. This paper has the primary objective of covering the formulation involving large displacements (geometrically nonlinear formulation), thus temporarily neglecting the latter two aspects. However, the intention is also to have a formulation that can relatively easily be extended so as to include the remaining two aspects as well. For that reason the choice of the authors is to take advantage of the updated Lagrangian formulation using engineering strain and stress measures. The variable boundary conditions can be resolved by including contact algorithms in the formulation, while material nonlinearities are to be dealt with by updating the material constitutive law dependent on the current strain and/or strain rate.

An incremental step-by-step approach represents a usual solution strategy in the nonlinear analysis. It assumes that the solution for discrete time  $t$  is known, and seeks the solution at discrete time  $t + \Delta t$ , with a suitably chosen time increment  $\Delta t$ . The solution at each time  $t$ , i.e. the structure configuration, has to be determined so as to satisfy the equilibrium condition between the internal and external forces:

$${}^t \mathbf{F}_{int} = {}^t \mathbf{F}_{ext}, \quad (1)$$

where external forces,  $\mathbf{F}_{ext}$ , comprise all the externally applied (body, surface and point) forces as well as the inertia and damping forces in the dynamic analysis. The internal forces are given as [2, 6]:

$${}^t \mathbf{F}_{int} = \int_{V_t} \mathbf{B}_L^T \hat{\boldsymbol{\sigma}} dV_t, \quad (2)$$

with  $\mathbf{B}_L$  denoting the linear strain-displacement matrix and  $\hat{\boldsymbol{\sigma}}$  is the vector of actual, Cauchy stresses:

$$\hat{\boldsymbol{\sigma}}^T = [\sigma_{xx} \quad \sigma_{yy} \quad \sigma_{zz} \quad \sigma_{xy} \quad \sigma_{yz} \quad \sigma_{xz}], \quad (3)$$

The Cauchy stresses are calculated using the constitutive, Hooke's matrix,  $\mathbf{C}$ , and actual strains,  $\boldsymbol{\varepsilon}$ , as:

$$\boldsymbol{\sigma} = \mathbf{C} \boldsymbol{\varepsilon}, \quad (4)$$

where both  $\boldsymbol{\sigma}$  and  $\boldsymbol{\varepsilon}$  are in the vector (Voigt) notation analogous to the form in Eq. (3).

The main issue now is determination of strains in the current structural configuration. There are different approaches to this problem, ranging from introduction of auxiliary strain measures (i.e. Green-Lagrange strain measure) up to introduction of an auxiliary "co-rotational" coordinate system. The approach applied in the present formulation determines engineering strains with respect to the global Cartesian coordinate system using the strain-displacement matrix for midpoint geometry,  $\mathbf{B}_{L/2}$ , for the calculation of incremental strains. Hence, having calculated displacement increment over time step,  $\Delta \mathbf{u}$ , the midpoint configuration between configurations  $\mathbf{x}_{n-1}$  and  $\mathbf{x}_n$  is given as:

$$\mathbf{x}_{1/2} = \mathbf{x}_{n-1} + \frac{\Delta \mathbf{u}}{2}, \quad (5)$$

The strain increment due to incremental displacements  $\Delta \mathbf{u}$  is then:

$$\Delta \boldsymbol{\varepsilon} = \mathbf{B}_{L/2} \Delta \mathbf{u}, \quad (6)$$

This method is an excellent approximation to the logarithmic strain if the strain steps are less than 10% [1]. It is at first simply added to the overall strain field in the previous configuration and in the next step it is necessary to decompose the overall motion over the time step into the rigid-body and deformable motion and to rotate the so-calculated strains through the rigid-body motion. This is done through polar decomposition of deformation gradient matrix:

$$\mathbf{F} = \begin{bmatrix} 1 + \Delta u_{,x} & u_{,y} & u_{,z} \\ v_{,x} & 1 + \Delta v_{,y} & v_{,z} \\ w_{,x} & w_{,y} & 1 + \Delta w_{,z} \end{bmatrix} = \mathbf{R} \mathbf{U}, \quad (7)$$

where  $\mathbf{R}$  is a proper orthogonal tensor representing rigid-body rotation and  $\mathbf{U}$  is called the right stretching tensor. The polar decomposition is performed starting from the right Cauchy-Green tensor,  $\mathbf{C}$ :

$$\mathbf{C} = \mathbf{F}^T \mathbf{F} = \mathbf{U} \mathbf{R}^T \mathbf{R} \mathbf{U} = \mathbf{U}^2, \quad (8)$$

the square root of which is obviously the stretching tensor. Since  $\mathbf{U}$  is a symmetric positive definite tensor it may be expressed in the spectral form:

$$\mathbf{U} = \sum_{i=1}^3 \lambda_i \mathbf{m}_i \otimes \mathbf{m}_i \quad i = 1, 2, 3, \quad (9)$$

$\lambda_i$  are called the principle stretches of the deformation and are determined in practice by taking the square root of the eigenvalues of  $\mathbf{C}$ ,  $\mathbf{m}_i$  are three mutually perpendicular unit

vectors obtained as the normalized eigenvectors of  $\mathbf{C}$  and  $\otimes$  stands for the dyadic product. The rotation tensor is from Eq. (7) given in a straightforward manner as:

$$\mathbf{R} = \mathbf{F} \mathbf{U}^{-1}, \quad (10)$$

and finally the strains in the last determined configuration with respect to the global c. s. are:

$$\boldsymbol{\varepsilon}_n = \mathbf{R}(\boldsymbol{\varepsilon}_{n-1} + \Delta\boldsymbol{\varepsilon})\mathbf{R}^T, \quad (11)$$

### 3. LINEAR TETRAHEDRAL ELEMENT

The decision to develop a tetrahedral element was driven by the fact that geometry of soft tissues is typically obtained by CT-scans (computer tomography) and is represented through surface triangularization. The requirement for high numerical efficiency was decisive for developing a relatively simple linear element capable of representing rigid-body and constant strain modes only, but with all necessary element vectors and matrices having a constant value over the domain of the element, thus not requiring their multiple evaluations at different integration points for the calculation.

The geometry of the element and degrees of freedom with respect to the global coordinates are depicted in Fig. 1.

For the derivation of the stiffness matrix of the element local coordinates (also known as natural coordinates) are used. They are defined so as to have the value 1 in the corresponding node and are equal to zero over the opposite surface of the tetrahedron, thus:

$$\zeta_L \in [0, 1] \quad L = 1, \dots, 4, \quad (12)$$

Of course, only three coordinates are independent of each other and the fourth can be determined using the condition:

$$\zeta_1 + \zeta_2 + \zeta_3 + \zeta_4 = 1, \quad (13)$$

And the shape functions are now simply defined as:

$$N_L = \zeta_L \quad L = 1, \dots, 4, \quad (14)$$

which provides at the same time the condition that the sum of the shape functions should be equal to 1. The relation between the Cartesian and the local tetrahedral coordinates is given by the matrix comprising global positions of the four nodes:

$$\begin{bmatrix} x \\ y \\ z \\ 1 \end{bmatrix} = \begin{bmatrix} x_1 & x_2 & x_3 & x_4 \\ y_1 & y_2 & y_3 & y_4 \\ z_1 & z_2 & z_3 & z_4 \\ 1 & 1 & 1 & 1 \end{bmatrix} \begin{bmatrix} \zeta_1 \\ \zeta_2 \\ \zeta_3 \\ \zeta_4 \end{bmatrix} = \mathbf{H} \begin{bmatrix} \zeta_1 \\ \zeta_2 \\ \zeta_3 \\ \zeta_4 \end{bmatrix}, \quad (15)$$

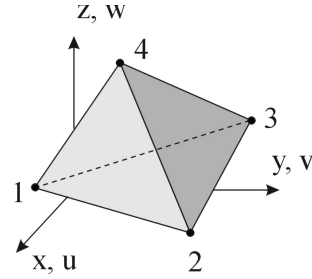


Fig. 1 4-nodes Tetrahedral Element



The geometrical stiffness matrix is given by:

$$\mathbf{K}_\sigma = \int_{V_t} \mathbf{B}_\sigma^T \boldsymbol{\sigma} \mathbf{B}_\sigma dV_t, \quad (22)$$

where matrix  $\mathbf{B}_\sigma$  is defined so that its product with the vector of nodal displacements,  $\tilde{\mathbf{u}}$ , gives all displacement partial derivatives  $[u_{,x} \ u_{,y} \ u_{,z} \ v_{,x} \ \dots \ w_{,z}]$ , thus having the following form:

$$\mathbf{B}_\sigma = \begin{bmatrix} \tilde{\mathbf{B}}_\sigma & \tilde{\mathbf{0}} & \tilde{\mathbf{0}} \\ \tilde{\mathbf{0}} & \tilde{\mathbf{B}}_\sigma & \tilde{\mathbf{0}} \\ \tilde{\mathbf{0}} & \tilde{\mathbf{0}} & \tilde{\mathbf{B}}_\sigma \end{bmatrix}. \quad (23)$$

$$\text{with: } \tilde{\mathbf{B}}_\sigma = \begin{bmatrix} N_{1,x} & 0 & 0 & N_{2,x} & \dots & N_{4,x} \\ N_{1,y} & 0 & 0 & N_{2,y} & \dots & N_{4,y} \\ N_{1,z} & 0 & 0 & N_{2,z} & \dots & N_{4,z} \end{bmatrix} \quad \text{and} \quad \tilde{\mathbf{0}} = \begin{bmatrix} 0 \\ 0 \\ 0 \end{bmatrix}, \quad (24)$$

while the matrix of Cauchy stresses,  $\boldsymbol{\sigma}$ , yields:

$$\boldsymbol{\sigma} = \begin{bmatrix} \tilde{\boldsymbol{\sigma}} & \bar{\mathbf{0}} & \bar{\mathbf{0}} \\ \bar{\mathbf{0}} & \tilde{\boldsymbol{\sigma}} & \bar{\mathbf{0}} \\ \bar{\mathbf{0}} & \bar{\mathbf{0}} & \tilde{\boldsymbol{\sigma}} \end{bmatrix}, \quad (25)$$

$$\text{with } \tilde{\boldsymbol{\sigma}} = \begin{bmatrix} \sigma_{11} & \sigma_{12} & \sigma_{13} \\ \sigma_{21} & \sigma_{22} & \sigma_{23} \\ \sigma_{31} & \sigma_{32} & \sigma_{33} \end{bmatrix} \quad \text{and} \quad \bar{\mathbf{0}} = \begin{bmatrix} 0 & 0 & 0 \\ 0 & 0 & 0 \\ 0 & 0 & 0 \end{bmatrix}. \quad (26)$$

Since all the above given matrices are constant over the domain of the element the Eqs. (2), (20) and (22) come down to the following simplified form:

$$\mathbf{F}_{int} = \mathbf{B}_L^T \hat{\boldsymbol{\sigma}} V_t, \quad \mathbf{K}_L = \mathbf{B}_L^T \mathbf{C} \mathbf{B}_L V_t \quad \text{and} \quad \mathbf{K}_\sigma = \mathbf{B}_\sigma^T \boldsymbol{\sigma} \mathbf{B}_\sigma V_t, \quad (27)$$

$$\text{where} \quad V_t = \frac{1}{6} \det \mathbf{H} \quad (28)$$

#### 4. VALIDATION OF THE ELEMENT AND FORMULATION

The main objective of this section is the validation of the developed element and the applied formulation. Results obtained by means of commercial software packages ANSYS and ABAQUS as well as experimental results will serve as a reference for the validation. The validation will be performed through a set of static examples, since the calculation of the tangential stiffness matrix and the vector of internal forces remains the main issue in the geometrically nonlinear formulation. The set of examples will go from very simple ones involving only one element and toward more complex examples involving a collection of elements.

The intention of the authors in the future is to use the element for transient calculations in combination with an explicit time integration scheme. Such a forward-marching scheme requires a time step smaller than a critical one (conditional stability) but the calculation is done without the Newton-Raphson iteration over the equilibrium. For that reason, the static cases considered in the paper will be calculated in a similar manner - small load increments will be applied allowing to proceed without the Newton-Raphson iteration and reaching a satisfying accuracy as the size of the load increment is reduced. This approach provides balancing between numerical effort and achieved accuracy.

#### 4.1. Single Element Test Cases

The first set of tests will be performed considering only one tetrahedral element exposed to a specific set of loads. The results from the developed element will be compared to those obtained with SOLID45-element from the ANSYS library of elements, which is originally an 8-node hexahedral element, but can be reduced to a tetrahedral one through a specific node numeration.

Isotropic material properties with Young's modulus  $E=1000 \text{ N/mm}^2$  and Poisson's coefficient  $\nu=0.3$  are chosen. The element has the configuration with one of the nodes at the origin of the global coordinate system and the remaining three nodes are located on the coordinate axes at a unity distance from the origin (Fig. 2). In the below considered cases the three nodes in the  $xy$ -plane are fixed, while the force acts at the node lying on the  $z$ -axis at a unity distance from the origin.

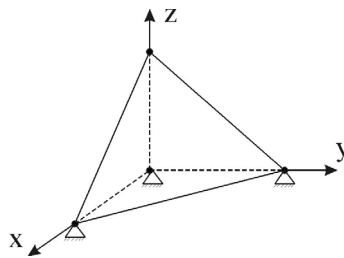


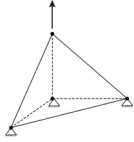
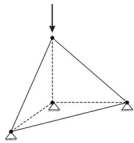
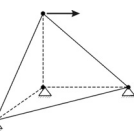
Fig. 2 Single Element with Constraints

In the first two cases the force acts along the  $z$ -axis, once as a tensile force and in the second case as a compressive one. The load is chosen so that no rotation of strains and stresses throughout the deformation is caused. Consequently, the cases serve as a verification of the approach based on the midpoint configuration to approximate the logarithmic strain (Eqs. (5) and (6)). The geometrically nonlinear results are summarized in the first two rows of Tab. 1. As already emphasized, the accuracy of the obtained results strongly depends on the size of the load increment (due to the lack of the Newton-Raphson iteration) and, of course, gets improved as the number of load increments is increased. The comparison with the results from the SOLID45-element demonstrates an agreement of the results that is quite satisfying. In the case of tensile force, the results are given for the nonlinear calculation performed with the highest number of load increments that was used, i.e. for 100 incremental steps. The case with compressive force demonstrates, however, that the calculation with 50 load increments provides a similar degree of accuracy.

In the third single element test case, the force acts along the y-axis, thus inducing shearing strains and stresses only. Besides the midpoint configuration approach for the approximation of the logarithmic strains, the rigid body rotation of strains becomes in this example an important issue as well. The third row in Tab. 1 shows once again a good agreement with the results from ANSYS, although the element and formulation presented in the paper are used with only 10 load increments.

It should be emphasized that both elements yield exactly the same linear solution for all the considered cases and they are 0.446 mm (tensile force), -0.446 mm (compressive force), 0.78 mm (shear), respectively. The comparison of the linear and nonlinear results shows the difference of up to 24%.

Table 1 Results of the Test Cases with a Single Element

Force		Displacement [mm] in the force direction	
Case	F [N]	ANSYS	Present (Increments)
	100 (tensile)	0.5616	0.55858 (100)
	100 (compressive)	-0.3596	-0.3622 (50)
	50	0.8635	0.8684 (10)

#### 4.2. Test Cases with a Cube

After the test cases with the single element, the next step is to verify the code when a number of elements are used to model an object. A set of simple test cases involving a cube discretized by five tetrahedral elements is considered. The length of the cube edge is equal to 1 and the material properties are the same as in the previous group of test cases. Following the same pattern established in the previous subsection, three cases are set. In each single case, the four nodes sited in the xy-plane are fixed, while the remaining four nodes are exposed to the concentrated forces of the same magnitude and direction. The cases differ from each other by the magnitude and direction of the applied forces. It should be emphasized that, due to the rough discretization, the FE model does not reflect the actual symmetry of the considered cases, which will also be obvious from the obtained results. The main objective is the verification of the element and formulation and it is achieved comparing the obtained results with those from exactly the same models made in commercial FEA software packages. At this point the quality of the models is not a subject of interest and the authors are aware that representative results for



the considered cube would require a significantly finer mesh. The here considered discretization of the cube is depicted in Fig. 3.

Tab. 2 gives the comparison of the obtained results with the results from ANSYS and ABAQUS. Opposite to the element from ANSYS, which is reduced from a hexahedral element, the element from ABAQUS (denoted as C3D4) is a genuine linear tetrahedral element. Once again, in the linear analysis the obtained results are the same and the geometrically nonlinear results from the present formulation are in high agreement with the results from the commercial software packages.

The first row in Tab. 2 exemplifies the change in achieved accuracy when the number of increments is reduced from 100 to 50. It actually shows that an acceptable accuracy may be obtained even with a smaller number of increments than used in performed calculations, although the Newton-Raphson iteration was not applied. Of course, one needs to be aware of the fact that there is a certain limit in the size of increment, after which the Newton-Raphson iteration would be necessary in order to reach an acceptable accuracy.

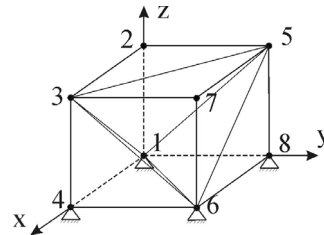
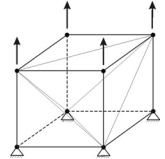
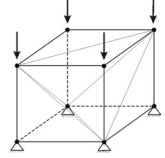
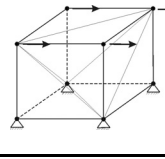


Fig. 3 Cube Discretized by 5 Tetrahedral Elements

Table 2 Results of the Test Cases with a Cube Discretized with 5 Tetrahedral Elements

Force		Displacement [mm] in the force direction			
Case	F [N]	ANSYS	ABAQUS	Present	Increments
	100	2, 7: 0.789	2, 7: 0.788	2, 7: 0.787 3, 5: 0.408	100
		3, 5: 0.419	3, 5: 0.419	2, 7: 0.774 3, 5: 0.405	50
	-100	2, 7: -0.408	2, 7: -0.409	2, 7: -0.411	50
		3, 5: -0.202	3, 5: -0.200	3, 5: -0.204	
	50	2: 0.853 3: 0.649 5: 0.732 7: 0.763	2: 0.860 3: 0.652 5: 0.737 7: 0.766	2: 0.862 3: 0.650 5: 0.739 7: 0.766	50

### 4.3. Comparison with Experimental Results on a Foam Sample

Finally, the element and formulation are tested using experimental results on a foam sample, which was exposed to a vertical force of  $F=6.585$  N exerted by a bar, as shown in Fig. 4. For the purpose of measuring the induced deformation the sample was provided with a grid.

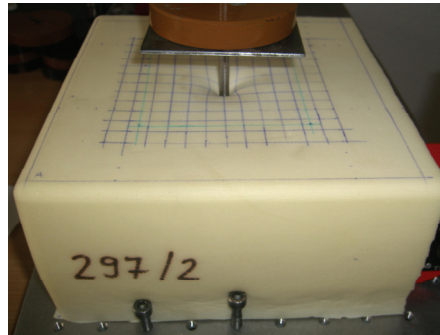


Fig. 4 Foam Sample under Vertical Force

In the calculation the foam is treated as a linearly elastic material with the measured Young's modulus of  $E=0.052 \text{ N/mm}^2$  [3], which is of the same order of magnitude encountered with soft tissues of internal organs. The Poisson's coefficient was not determined in measurements and it is assumed to be  $\nu=0.3$ . The calculation is performed with the developed element and in ANSYS.

The results from ANSYS are presented in Fig. 5a. The maximal value of calculated displacement is 9.77 mm, while in the experiment it is 9 mm. It can also be noticed that the shape of the funnel determined by experiment is somewhat wider than the one yielded by the calculation. Both differences can be attributed to the fact that the surface of the sample is covered by a kind of a "skin" (a consequence of the production process), which is not accounted for in the calculation, the fact that the Poisson's coefficient was not experimentally determined but assumed, and finally, the assumption of linearly elastic material behavior, which is only a rough approximation of the real behavior.

The results from the developed element and formulation are given in Fig. 5b. They are obtained using 20 load increments and it can be noticed that they are very similar to the results from ANSYS. Generally, it can be said that the calculated results give a satisfying representation of the measured deformation.

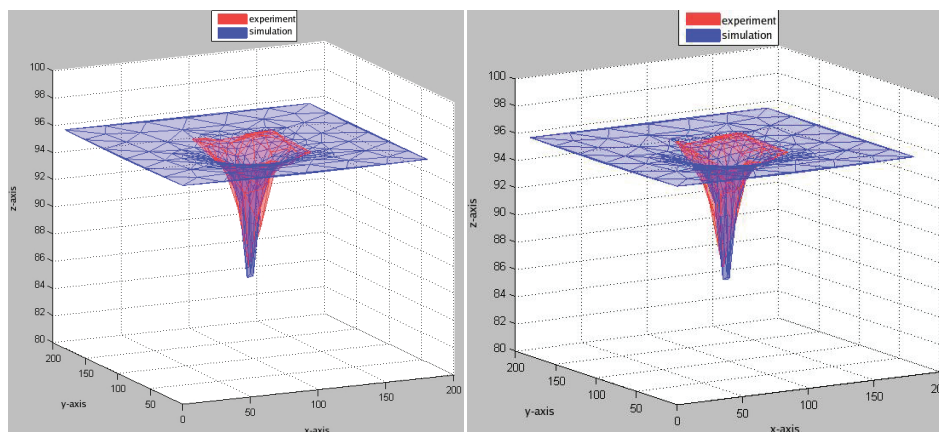


Fig 5 Foam Sample - Comparison between Experimental Results and Calculation:  
 a) ANSYS  
 b) Present Formulation

## 5. CONCLUSIONS

The paper describes a linear tetrahedral element developed for geometrically nonlinear analysis. The primary objective of the development is its application to modeling deformational behavior of soft tissues. The updated Lagrangian formulation is used. The proposed solution procedure proceeds without the Newton-Raphson iteration, thus resembling the approach used in explicit time integration schemes, and it could be noticed that the obtained results converge toward the results from the commercial FEA codes as the size of the increment is reduced. This offers a simple way of performing a trade-off between the computational effort and accuracy. One of the tasks that the here presented tool can certainly be used for is development of finite element models with the aim to validate models based on other approaches and used for real-time simulations in simulators (e.g. mass-spring system). Furthermore, the formulation provides a good basis for modifications with the aim to get an FEM formulation capable of real-time simulation. This task is a real challenge and the authors have already made first steps in this direction, which will be presented in future publications.

## REFERENCES

1. *Ansys Theory Reference* (available at: [http://www1.ansys.com/customer/content/documentation/90/ansys/a\\_thry90.pdf](http://www1.ansys.com/customer/content/documentation/90/ansys/a_thry90.pdf))
2. Bathe, K. J., 1982, *Finite element procedures in engineering analysis*, Prentice-Hall, Inc., Englewood Cliffs, New Jersey, 733 p.
3. Jöchen, K., 2006, *Entwicklung und Testung einfacher mechanischer Organmodelle für die virtuelle Laparoskopie*, Diplom thesis, Otto-von-Guericke Universität, Magdeburg.
4. Kuhn, Ch., Kühnapfel, U., Deussen, O., 1995, *Echtzeitsimulation deformierbarer Objekte zur Ausbildungsunterstützung in der Minimal-Invasiven Chirurgie*, GI Workshop Modelling – Virtual Worlds – Distributed Graphics, Proc. Int. Workshop MVD'95, Bad Honnef.
5. Kühnapfel, U. G., Kuhn, C., Hübner, M., Krumm, H. G., Maa, E. H., Neisius, B., 1997, *The Karlsruhe Endoscopic Surgery Trainer as an example for virtual reality in medical education*, Minimally Invasive Therapy and Allied Technologies, No. 6, pp. 122-125.
6. Marinković D., Köppe H., Gabbert U.: *Finite Element Development for Generally Shaped Piezoelectric Active Laminates, part II – Geometrically Nonlinear Approach*, The Scientific journal Facta Universitatis, Series Mechanical Engineering, Vol. 3, N<sup>o</sup> 1, University of Niš, Niš, 2005., pp. 1 ÷ 16
7. Picinbono, G., Delingette, H., and Ayache, N., 2001, *Non-linear and anisotropic elastic soft tissue models for medical simulation*. In ICRA2001: IEEE International Conference Robotics and Automation, Seoul Korea.
8. Zhang, M., Zheng, Y.P., Mak, A.F.T., 1997, *Estimating the effective Young's modulus of soft tissues from indentation tests – nonlinear finite element analysis of effects of friction and large deformation*. Med. Eng. Phys. Vol. 19, No. 6, pp. 512-517.

## EFIKASNA GEOMETRIJSKI NELINEARNA FE-FORMULACIJA ZA ANALIZU DEFORMACIJA MEKIH MATERIJALA

**Dragan Marinković, Katja Joechen**

*Precizno određivanje deformacije mekih tela je zahtevan zadatak, jer uključuje i geometrijski i materijalno nelinearno ponašanje, kao i promenljive granične uslove, odnosno probleme kontakta. Rad predstavlja prvi korak autora u ovladavanju ovom problematikom i opisuje razvoj efikasnog 3D konačnog elementa za modeliranje geometrijski nelinearnih deformacija. Predložena geometrijski*

*nelinearna formulacija je tipa updated Lagrange i može se relativno lako proširiti tako da uzme u obzir i druge aspekte nelinearnog ponašanja (materijalnu nelinearnost, kontakt). Ona, takođe, predstavlja dobar kompromis između potrebnog numeričkog napora i ostvarene tačnosti analize. Skup primera, počev od vrlo jednostavnih i idući ka složenijim, je dat sa ciljem da se prikaže primena razvijenog elementa i formulacije.*

**Ključne reči:** *metoda konačnih elemenata, geometrijski nelinearna analiza, tetraedar element*